Yaseen et al. *Advances in Difference Equations* (2021) 2021:210
https://doi.org/10.1186/s13662-021-03360-6

Advances in Difference Equations
a SpringerOpen Journal

RESEARCH **Open Access**

A collocation method based on cubic trigonometric B-splines for the numerical simulation of the time-fractional diffusion equation

Muhammad Yaseen[1], Muhammad Abbas[1*] and Muhammad Bilal Riaz[2,3]

*Correspondence: muhammad.abbas@uos.edu.pk
[1]Department of Mathematics, University of Sargodha, 40100 Sargodha, Pakistan
Full list of author information is available at the end of the article

Abstract

Fractional differential equations sufficiently depict the nature in view of the symmetry properties, which portray physical and biological models. In this paper, we present a proficient collocation method based on cubic trigonometric B-Splines (CuTBSs) for time-fractional diffusion equations (TFDEs). The methodology involves discretization of the Caputo time-fractional derivatives using the typical finite difference scheme with space derivatives approximated using CuTBSs. A stability analysis is performed to establish that the errors do not magnify. A convergence analysis is also performed The numerical solution is obtained as a piecewise sufficiently smooth continuous curve, so that the solution can be approximated at any point in the given domain. Numerical tests are efficiently performed to ensure the correctness and viability of the scheme, and the results contrast with those of some current numerical procedures. The comparison uncovers that the proposed scheme is very precise and successful.

Keywords: Time-fractional diffusion equation; Cubic trigonometric B-spline method; Spline approximations; Stability; Convergence

1 Introduction

The time-fractional diffusion equation (TFDE) is given as

$$ {}_a^C D_t^\gamma u(s,t) - \frac{\partial^2}{\partial s^2} u(s,t) = f(s,t), \quad 0 < \gamma < 1, \tag{1} $$

subject to the following initial condition (IC) and boundary conditions (BCs):

$$ u(s,0) = \varphi(s), \quad a \le s \le b, \tag{2} $$

$$ u(a,t) = \psi_1(t), \qquad u(b,t) = \psi_2(t), \quad t \ge 0, \tag{3} $$

where the diffusion exponent is denoted by γ, and ${}_a^C D_t^\gamma u(s,t)$ is the Caputo fractional derivative (CFD) of order γ given by [1]

$$ {}_a^C D_s^\gamma f(s) = J^{n-\gamma} D^n f(s) = \begin{cases} \frac{1}{\Gamma(n-\gamma)} \int_a^s \frac{f^{(n)}(\xi)}{(s-\xi)^{\gamma+1-n}}\, d\xi, & n-1 < \gamma < n \in \mathbb{N}, \\ \frac{d^n}{ds^n} f(s), & \gamma = n \in \mathbb{N}. \end{cases} \tag{4} $$

Note that $\gamma = 0$ and $\gamma = 1$ correspond to the classical Helmholtz and standard diffusion equations, respectively.

The fractional calculus [1–3] has gained keenness in numerous fields such as chemistry, plasma physics, material science, biology, fluid mechanics, and so on. The fractional-order differential and integral equations are reliable tools to describe physical models of interest more exactly than their integer-order counterparts. A variety of applications of fractional calculus and TFDEs can be found in [3–10]. The numerical and approximate solutions play an important role in exploring applications of fractional partial differential equations. It is emphasized in many research papers that the fractional derivatives and integrals are more efficient tools for modeling the hereditary and memory effects of different processes and materials, in contrast with integer-order models, in which such effects are ignored.

Numerous analytical schemes are available for TFDEs [1, 11–13]. Numerical techniques are developed continuously because exact solutions are available in very few cases. Numerous numerical procedures for solving TFDEs have been developed recently. Esmaeili and Garrappa [14] obtained numerical solutions of TFDEs by a pseudospectral scheme. Mustapha et al. [15] presented a discontinuous Petrov–Galerkin method for TFDEs. Zhuang and Liu [16] obtained implicit difference approximations for TFDEs. Karatay et al. [17] used the Crank–Nicholson approach to construct a scheme for TFDEs. A weighted average and explicit finite difference schemes were developed in [18, 19] for TFDEs. Murio [20] presented an unconditionally stable implicit scheme for TFDEs on a finite slab. Tasbozan et al. [21] introduced a numerical scheme using B-spline basis functions for space fractional subdiffusion equations. Huang et al. [22] presented a fully discrete discontinuous Galerkin method for TFDEs. Chen et al. [23] used the Fourier method to find approximate solutions of the fractional diffusion equation describing subdiffusion. Gao and Sun [24] presented a compact finite difference scheme for fractional subdiffusion equations using a compact finite difference scheme.

In this paper, we present a cubic trigonometric B-spline collocation method to obtain numerical solutions of TFDEs. The main motivation behind using B-splines is that the solutions are obtained in the form of piecewise continuous sufficiently smooth functions, enabling us to approximate the solution at any desired location in the domain. The stability and convergence analysis are also discussed to establish that the scheme does not propagate errors. Numerical tests are performed to affirm the feasibility and applicability of the method. The results are compared with those presented in [22, 23].

The rest of the paper is organized as follows. In Sect. 2, we derive a numerical procedure. The stability and convergence analysis of the scheme are presented in Sects. 3 and 4, respectively. In Sect. 5, we show a contrast of our numerical results with those of [22, 23]. Section 6 contains the outcomes of this study.

2 Materials and methods

2.1 Space discretization

Let the solution domain be $[a,b] \times [0,T]$. For given positive integers M and N, let $\tau = \frac{T}{N}$ be the temporal and $h = \frac{b-a}{M}$ the spatial step sizes, respectively. The space interval $[a,b]$ is uniformly partitioned as $a = s_0 < s_1 < \cdots < s_M = b$, where $s_i = a + ih$, $i = 0,\ldots,M$. In this partition, the CuTBS function $TB_i^4(x)$ [25] is defined as

$$TB_i^4(s) = \frac{1}{\beta}\begin{cases} \sigma^3(s_i), \\ \quad s \in [s_i, s_{i+1}], \\ \sigma(s_i)(\sigma(s_i)\varphi(s_{i+2}) + \varphi(s_{i+3})\sigma(s_{i+1})) + \varphi(s_{i+4})\sigma^2(s_{i+1}), \\ \quad s \in [s_{i+1}, s_{i+2}], \\ \varphi(s_{i+4})(\sigma(s_{i+1})\varphi(s_{i+3}) + \varphi(s_{i+4})\sigma(s_{i+2})) + \sigma(s_i)\varphi^2(s_{i+3}), \\ \quad s \in [s_{i+2}, s_{i+3}], \\ \varphi^3(s_{i+4}), \\ \quad s \in [s_{i+3}, s_{i+4}], \end{cases} \tag{5}$$

where

$$\sigma(s_i) = \sin\left(\frac{s - s_i}{2}\right), \qquad \varphi(s_i) = \sin\left(\frac{s_i - s}{2}\right), \qquad \beta = \sin\left(\frac{h}{2}\right)\sin(h)\sin\left(\frac{3h}{2}\right).$$

The support of the B-spline function $TB_i^4(s)$ is assumed to be $[s_i, s_{i+4}]$. Note that each TB_i^4 is piecewise cubic and nonzero over four consecutive subintervals and vanishes otherwise. Consequently, each subinterval $[s_i, s_{i+1}]$ contains three segments of $TB_i^4(s)$. Suppose that $u(s,t)$ and $U(s,t)$ are the analytic and numerical solutions of the given differential equation. We seek the approximation $U(s,t)$ to the solution $u(s,t)$ in terms of TB_i^4 as [26, 27]

$$u(s,t) \simeq U(s,t) = \sum_{i=-1}^{M+1} c_i(t) TB_i^4(s), \tag{6}$$

where $c_i(t)$ are unknowns, which are to be determined using the collocation method by utilizing the initial and boundary conditions. Using (5) and (6), the values of $U(x,t)$ and its necessary derivatives at the nodal points are determined in terms of the parameters c_i as follows:

$$\begin{cases} U(s_i,t) = \varrho_1 c_{i-1}(t) + \varrho_2 c_i(t) + \varrho_1 c_{i+1}(t), \\ U_s(s_i,t) = -\varrho_3 c_{i-1}(t) + \varrho_3 c_{i+1}(t), \\ U_{ss}(s_i,t) = \varrho_4 c_{i-1}(t) + \varrho_5 c_i(t) + \varrho_4 c_{i+1}(t), \end{cases} \tag{7}$$

where

$$\varrho_1 = -\frac{1}{2\sin(h)\sin(\frac{3h}{2})}\big(\cos(h) - 1\big),$$

$$\varrho_2 = -\frac{2}{4\sin^2(\frac{h}{2}) - 3},$$

$$\varrho_3 = \frac{3}{4\sin(\frac{3h}{2})},$$

$$\varrho_4 = \frac{3}{4}\left(\frac{3\sin^2(\frac{h}{2}) - 2}{\sin^2(\frac{h}{4}) - \sin^2(\frac{5h}{4})}\right),$$

$$\varrho_5 = -\frac{3}{(4\cos(h) + 2)(\tan^2(\frac{h}{2}))}.$$

2.2 Temporal discretization

To discretize the problem in time scale, we take the uniform partition on $[0, T]$ as $0 = t_0 < t_1 < t_2 < \cdots < t_N = T$ with $\tau = t_{n+1} - t_n$ for $n = 0, 1, \ldots, N-1$. Following [28], the CFD ${}_a^C D_t^\gamma u(s,t)$ is discretized as

$$\begin{aligned} {}_a^C D_t^\gamma u(s,t_{n+1}) &= \sum_{l=0}^{n} \kappa_l \frac{u(s,t_{n+1-l}) - u(s,t_{n-l})}{\Gamma(2-\gamma)\tau^\gamma} + r_\tau^{n+1} \\ &= \frac{1}{\alpha_0}\left(u(s,t_{n+1}) - \sum_{l=0}^{n-1}(\kappa_l - \kappa_{l+1})u(s,t_{n-l}) - \kappa_n u(s,t_0)\right) + r_\tau^{n+1} \\ &= \frac{1}{\alpha_0}\left(u^{n+1} - \sum_{l=0}^{n-1}(\kappa_l - \kappa_{l+1})u^{n-l} - \kappa_n u^0\right) + r_\tau^{n+1}, \end{aligned} \tag{8}$$

where $u^n = u(s,t_n)$, $\alpha_0 = \tau^\gamma \Gamma(2-\gamma)$, $\kappa_l = (l+1)^{1-\gamma} - l^{1-\gamma}$, and r_τ^{n+1} is the truncation error. Note that

$$\begin{cases} \kappa_l > 0, \quad l = 0, 1, 2, \ldots, N, \\ 1 = \kappa_0 > \kappa_1 > \kappa_2 > \cdots > \kappa_l \quad \text{and} \quad \kappa_l \to 0 \quad \text{as } l \to \infty, \\ \sum_{l=0}^{N-1}(\kappa_l - \kappa_{l+1}) + \kappa_N = 1. \end{cases} \tag{9}$$

It is shown in [29] that r_τ^{n+1} satisfies

$$r_\tau^{n+1} \leq C_u \tau^{2-\gamma},$$

where the constant C_u depends on u. Inserting (8) into (1) gives

$$u^{n+1} - \sum_{l=0}^{n-1}(\kappa_l - \kappa_{l+1})u^{n-l} - \kappa_n u^0 - \alpha_0 \left(u^{n+1}\right)_{ss} = \alpha_0 f^{n+1}. \tag{10}$$

To obtain a full discretization, let $c_i^n = c_i(t_n)$ and $U_i^n = U(s_i, t_n)$ for $i = 0, 1, \ldots, M$, $n = 0, 1, \ldots, N$. Now substituting (6) and (7) into (10), we get

$$\begin{aligned} &(\varrho_1 - \alpha_0\varrho_4)c_{i-1}^{n+1} + (\varrho_2 - \alpha_0\varrho_5)c_i^{n+1} + (\varrho_1 - \alpha_0\varrho_4)c_{i+1}^{n+1} \\ &\quad = \sum_{l=0}^{n-1}(\kappa_l - \kappa_{l+1})\left(\varrho_1 c_{i-1}^{n-l} + \varrho_2 c_i^{n-l} + \varrho_1 c_{i+1}^{n-l}\right) + \kappa_n\left(\varrho_1 c_{i-1}^0 + \varrho_2 c_i^0 + \varrho_1 c_{i+1}^0\right) \\ &\qquad + \alpha_0 f\left(s_i, t^{n+1}\right). \end{aligned} \tag{11}$$

Framework (11) is a system of $(M+1)$ equations in $(M+3)$ unknowns. Then we use given boundary conditions to obtain two additional equations. Consequently, we obtain a consistent diagonal system, which can be solved using any suitable algorithm based on Gaussian elimination.

2.3 Initial vector

The initial vector $\mathbf{d}^0 = [d_{-1}^0, d_0^0, \dots, d_{M+1}^0]^T$ is required to commence the iterative process, which can be obtained using the IC and the derivatives of IC at the two boundaries as follows [30–38]:

1. $(u_i^0)_s = \frac{d}{ds}\varphi(s_i)$, $i = 0$,
2. $u_i^0 = \varphi(s_i)$, $i = 0, 1, \dots, M$,
3. $(u_i^0)_s = \frac{d}{ds}\varphi(s_i)$, $i = M$,

which becomes the matrix equation

$$Ad^0 = b, \tag{12}$$

where

$$A = \begin{bmatrix} -\varrho_3 & 0 & \varrho_3 & \cdots & \cdots & \cdots & \cdots & 0 \\ \varrho_1 & \varrho_2 & \varrho_1 & \ddots & & & & \vdots \\ 0 & \varrho_1 & \varrho_2 & \varrho_1 & \ddots & & & \vdots \\ \vdots & \ddots & \ddots & \ddots & \ddots & \ddots & & \vdots \\ \vdots & & \ddots & \ddots & \ddots & \ddots & \ddots & \vdots \\ \vdots & & & & \ddots & \varrho_1 & \varrho_2 & \varrho_1 \\ 0 & \cdots & \cdots & \cdots & \cdots & -\varrho_3 & 0 & \varrho_3 \end{bmatrix} \tag{13}$$

and $b = [\varphi'(s_0), \varphi(s_0), \dots, \varphi(s_M), \varphi'(s_M)]^T$.

3 Stability analysis

Here we test scheme (11) for the stability analysis. The Duhamels principle [39] states that for an inhomogeneous case, the stability estimates are the same as those of the corresponding homogeneous case. So we present the stability analysis only for the case $f = 0$. Let ω_i^n and $\tilde{\omega}_i^n$ be the growth factor and its approximation, respectively, of a Fourier mode. Defining $\Omega_i^n = \omega_i^n - \tilde{\omega}_i^n$, from (11) we get

$$\begin{aligned} &(\varrho_1 - \alpha_0\varrho_4)\Omega_{i-1}^{n+1} + (\varrho_2 - \alpha_0\varrho_5)\Omega_i^{n+1} + (\varrho_1 - \alpha_0\varrho_4)\Omega_{i+1}^{n+1} \\ &\quad = \sum_{l=0}^{n-1}(\kappa_l - \kappa_{l+1})\big(\varrho_1\Omega_{i-1}^{n-l} + \varrho_2\Omega_i^{n-l} + \varrho_1\Omega_{i+1}^{n-l}\big) \\ &\qquad + \kappa_n\big(\varrho_1\Omega_{i-1}^0 + \varrho_2\Omega_i^0 + \varrho_1\Omega_{i+1}^0\big). \end{aligned} \tag{14}$$

The initial and boundary conditions are satisfied as

$$\Omega_i^0 = 0, \quad i = 1, 2, \dots, M-1, \tag{15}$$

and

$$\Omega_0^n = \psi_1(t_n), \qquad \Omega_M^n = \psi_2(t_n), \quad n = 0, 1, \dots, N. \tag{16}$$

The grid function is defined as

$$\Omega^n(s) = \begin{cases} 0, & 0 < s \leq \frac{h}{2} \text{ or } (b-a) - \frac{h}{2} < s \leq (b-a), \\ \Omega_i^n, & s_i - \frac{h}{2} < s \leq s_i + \frac{h}{2}, i = 1, \dots, M-1. \end{cases}$$

The function $\Omega^n(s)$ has the Fourier expansion

$$\Omega^n(s) = \sum_{m=-\infty}^{\infty} \eta_n(m) e^{\frac{i2\pi ms}{b-a}}, \quad n = 0, 1, \dots, N,$$

where $\eta_n(m) = \frac{1}{b-a}\int_a^b \Omega^n(s) e^{\frac{-i2\pi ms}{b-a}}\,ds$. Let $\Omega^n = [\Omega_1^n, \Omega_2^n, \dots, \Omega_{M-1}^n]^T$ and

$$\|\Omega^n\|_2 = \left(\sum_{i=1}^{M-1} h\left|\Omega_i^n\right|^2\right)^{\frac{1}{2}} = \left[\int_a^b \left|\Omega^n(s)\right|^2 ds\right]^{\frac{1}{2}}.$$

Using the Parseval equality, we see that

$$\int_a^b \left|\Omega^n(s)\right|^2 ds = \sum_{m=-\infty}^{\infty} \left|\eta_n(m)\right|^2,$$

so that

$$\|\Omega^n\|_2^2 = \sum_{m=-\infty}^{\infty} \left|\eta_n(m)\right|^2. \tag{17}$$

Suppose that $\Omega_i^n = \eta_n e^{I\theta is}$ is the solution to system (14)–(15), where $I = \sqrt{-1}$ and $\theta \in [-\pi, \pi]$, so that equation (14) reduces to

$$\begin{aligned} &(\varrho_1 - \alpha_0\varrho_4)\eta_{n+1}e^{I\theta(i-1)s} + (\varrho_2 - \alpha_0\varrho_5)\eta_{n+1}e^{I\theta(i)s} + (\varrho_1 - \alpha_0\varrho_4)\eta_{n+1}e^{I\theta(i+1)s} \\ &\quad = \sum_{l=0}^{n-1}(\kappa_l - \kappa_{l+1})\big(\varrho_1\eta_{n-l}e^{I\theta(i-1)s} + \varrho_2\eta_{n-l}e^{I\theta(i)s} + \varrho_1\eta_{n-l}e^{I\theta(i+1)s}\big) \\ &\qquad + \kappa_n\big(\varrho_1\eta_0 e^{I\theta(i-1)s} + \varrho_2\eta_0 e^{I\theta is} + \varrho_1\eta_0 e^{I\theta(i+1)s}\big). \end{aligned} \tag{18}$$

Dividing (18) by $e^{I\theta is}$, using $e^{-I\theta s} + e^{I\theta s} = 2\cos(\theta s)$, and gathering like terms, we get

$$\left(1 - \frac{\alpha_0(2\cos(\theta s)\varrho_4 + \varrho_5)}{2\varrho_1\cos(\theta s) + \varrho_2}\right)\eta_{n+1} = \sum_{l=0}^{n-1}(\kappa_l - \kappa_{l+1})\eta_{n-l} + \kappa_n\eta_0. \tag{19}$$

Without loss of generality, let $\theta = 0$, so that the last equation reduces to

$$\left(1 - \frac{\alpha_0(2\varrho_4 + \varrho_5)}{2\varrho_1 + \varrho_2}\right)\eta_{n+1} = \sum_{l=0}^{n-1}(\kappa_l - \kappa_{l+1})\eta_{n-l} + \kappa_n\eta_0. \tag{20}$$

Then

$$\eta_{n+1} = \frac{1}{\zeta}\sum_{l=0}^{n-1}(\kappa_l - \kappa_{l+1})\eta_{n-l} + \frac{1}{\zeta}\kappa_n\eta_0, \tag{21}$$

where $\zeta = 1 - \frac{\alpha_0(2\varrho_4+\varrho_5)}{2\varrho_1+\varrho_2}$. Note that $\frac{\alpha_0(2\varrho_4+\varrho_5)}{2\varrho_1+\varrho_2} = -\frac{3\alpha_0}{4}\tan(\frac{h}{4})^2 \leq 0$, so that $\zeta \geq 1$.

Proposition 1 *If η_k $(k = 0, 1, \dots, N)$ is the solution of equation (21), then $|\eta_k| \leq |\eta_0|$.*

Proof We use induction on k. For $k = 0$, equation (21) gives $\eta_1 = \frac{1}{\zeta}\eta_0$, so that $|\eta_1| = \frac{1}{\zeta}|\eta_0| \leq |\eta_0|$ because $\zeta \geq 1$. Supposing $|\eta_i| \leq |\eta_0|$, $i = 1, 2, \dots, k$, from (21) we get

$$\begin{aligned}
|\eta_{k+1}| &\leq \frac{1}{\zeta}\sum_{l=0}^{k-1}(\kappa_l - \kappa_{l+1})|\eta_{n-l}| + \frac{1}{\zeta}\kappa_k|\eta_0| \\
&\leq \sum_{l=0}^{k-1}(\kappa_l - \kappa_{l+1})|\eta_0| + \kappa_k|\eta_0| \\
&= |\eta_0|\left(\sum_{l=0}^{k-1}(\kappa_l - \kappa_{l+1}) + \kappa_k\right) \\
&= |\eta_0|.
\end{aligned} \tag{22}$$

□

Theorem 1 *Scheme (11) is unconditionally stable.*

Proof By Proposition 1 and relation (17) we have

$$\left\|\Omega^k\right\|_2 \leq \left\|\Omega^0\right\|_2, \quad k = 0, 1, \dots, N,$$

which establishes the unconditional stability. □

4 Convergence analysis

Here we give convergence estimates for the discrete-time problem (10). As in the case of stability analysis, we present the convergence analysis for the homogeneous problem only.

Theorem 2 *Let $\{u(s,t^n)\}_{n=0}^{N-1}$ be the exact solution of (1), and let $\{u^n\}_{n=0}^{N-1}$ be the discrete-time solution of (10). Then*

$$\left\|e^{n+1}\right\| \leq D + C_u\tau^{2-\gamma},$$

where $e^{n+1} = u(s,t^{n+1}) - u^{n+1}$, and D is a constant.

Proof As before, we give a proof for $f = 0$ only. Note that the exact solution u also satisfies the semidiscrete scheme (10), so that we have

$$u\left(s,t^{n+1}\right) = \sum_{l=0}^{n-1}(\kappa_l - \kappa_{l+1})u\left(s,t^{n-l}\right) + \kappa_n u\left(s,t^0\right) + \alpha_0\left(u\left(s,t^{n+1}\right)\right)_{ss} \tag{23}$$

and

$$u^{n+1} = \sum_{l=0}^{n-1} (\kappa_l - \kappa_{l+1}) u^{n-l} + \kappa_n u^0 + \alpha_0 \left(u^{n+1}\right)_{ss}. \tag{24}$$

Subtracting (24) from (23), we obtain

$$\begin{aligned} e^{n+1} &= \sum_{l=0}^{n-1} (\kappa_l - \kappa_{l+1}) e^{n-l} + \kappa_n e^0 + \alpha_0 \left(e^{n+1}\right)_{ss} + r_\tau^{n+1} \\ &= \sum_{l=0}^{n-1} (\kappa_l - \kappa_{l+1}) e^{n-l} + \alpha_0 \left(e^{n+1}\right)_{ss} + r_\tau^{n+1}, \end{aligned} \tag{25}$$

where we have used the fact that $e^0 = 0$. Now taking the inner product of both sides of (25) with e^{n+1} and using $\langle x, x\rangle = \|x\|^2 \geq 0$, we get

$$\begin{aligned} \left\langle e^{n+1}, e^{n+1}\right\rangle &= \sum_{l=0}^{n-1} (\kappa_l - \kappa_{l+1}) \left\langle e^{n-l}, e^{n+1}\right\rangle + \alpha_0 \left\langle \left(e^{n+1}\right)_{ss}, e^{n+1}\right\rangle + \left\langle r_\tau^{n+1}, e^{n+1}\right\rangle \\ &= \sum_{l=0}^{n-1} (\kappa_l - \kappa_{l+1}) \left\langle e^{n-l}, e^{n+1}\right\rangle - \alpha_0 \left\langle \left(e^{n+1}\right)_{s}, \left(e^{n+1}\right)_{s}\right\rangle + \left\langle r_\tau^{n+1}, e^{n+1}\right\rangle \\ &= \sum_{l=0}^{n-1} (\kappa_l - \kappa_{l+1}) \left\langle e^{n-l}, e^{n+1}\right\rangle - \alpha_0 \left\| \left(e^{n+1}\right)_{s} \right\|^2 + \left\langle r_\tau^{n+1}, e^{n+1}\right\rangle \\ &\leq \sum_{l=0}^{n-1} (\kappa_l - \kappa_{l+1}) \left\langle e^{n-l}, e^{n+1}\right\rangle + \left\langle r_\tau^{n+1}, e^{n+1}\right\rangle, \end{aligned} \tag{26}$$

where we have used the relations $\langle u_{ss}, u\rangle = -\langle u_s, u_s\rangle$ and $\langle x, x\rangle = \|x\|^2$. Applying the Cauchy–Schwarz inequality $\langle x, y\rangle \leq \|x\| \|y\|$ in (26), we obtain

$$\left\|e^{n+1}\right\|^2 \leq \sum_{l=0}^{n-1} (\kappa_l - \kappa_{l+1}) \left\|e^{n-l}\right\| \left\|e^{n+1}\right\| + \left\|r_\tau^{n+1}\right\| \left\|e^{n+1}\right\|. \tag{27}$$

Dividing (27) throughout by $\|e^{n+1}\|$, we obtain

$$\begin{aligned} \left\|e^{n+1}\right\| &\leq \sum_{l=0}^{n-1} (\kappa_l - \kappa_{l+1}) \left\|e^{n-l}\right\| + \left\|r_\tau^{n+1}\right\| \\ &\leq D_n \sum_{l=0}^{n-1} (\kappa_l - \kappa_{l+1}) + \left\|r_\tau^{n+1}\right\| \\ &\leq D_n (1 - \kappa_n) + \left\|r_\tau^{n+1}\right\| \\ &\leq D + C_u \tau^{2-\gamma}, \end{aligned} \tag{28}$$

where $D_n = \max_{0 \leq l \leq n-1} \|e^{n-l}\|$ and $D = \max_{0 \leq n \leq N} D_n$. We have also used the relation $(1 - \kappa_n) < 1$. □

5 Numerical results and discussions

In this section, we present the results of the numerical tests for the TFDE (1) with initial (2) and boundary conditions (3). We use the following error norms to measure the accuracy of the method:

$$L_2 = \left\| U^{\text{exact}} - U^N \right\|_2 \simeq \sqrt{h \sum_{j=-1}^{M+1} \left(\left| U_j^{\text{exact}} - U_j^N \right| \right)^2}$$

and

$$L_\infty = \left\| U^{\text{exact}} - U^N \right\|_\infty \simeq \max_{-1 \le j \le M+1} \left| U_j^{\text{exact}} - U_j^N \right| |,$$

where U^{exact} is the exact solutions, and $(U_N)_j$ is the approximate one. The order of convergence is given by

$$OC = \frac{\log(\text{Error}(M)/\,\text{Error}(2M))}{\log(2M/M)},$$

where Error(M) and Error$(2M)$ are the L_∞ norms at M and $2M$, respectively.

Example 1 Consider the TFDE (1) [22] with initial condition $u(s,0) = \sin s$ and boundary conditions $u(0,t) = u(\pi,t) = 0$. This problem has the exact solution $u(s,t) = E_\gamma(-t^\gamma)\sin(s)$, where $E_\gamma(z) = \sum_{m=0}^{\infty} \frac{z^m}{\Gamma(\gamma m+1)}$ is the ML function. The corresponding source term is $f = 0$.

We apply the proposed algorithm (11) to the problem. The approximate solutions when $\tau = 0.01$, $h = \frac{\pi}{20}$, and $\gamma = 0.5$ at $t = 0.5$ and $t = 1$ are given by

$$U(s,0.5) = \begin{cases} 0.4361\cos(\frac{s}{2}) - 0.1707\cos^3(\frac{s}{2}) - 0.0618\sin^3(\frac{s}{2}) & \\ \quad + \sin(\frac{s}{2})(0.0762 + 0.2560\sin(s)) & \\ \quad + 0.0464\csc(\frac{s}{2})\sin^2(s), & s \in [0, \frac{\pi}{20}], \\ 0.0009\cos(\frac{s}{2}) - 0.0009\cos^3(\frac{s}{2}) - 0.1355\sin^3(\frac{s}{2}) & \\ \quad + \sin(\frac{s}{2})(0.6433 + 0.0014\sin(s)) & \\ \quad + 0.1016\csc(\frac{s}{2})\sin^2(s), & s \in [\frac{\pi}{20}, \frac{\pi}{10}], \\ 0.0047\cos(\frac{s}{2}) - 0.0046\cos^3(\frac{s}{2}) - 0.1426\sin^3(\frac{s}{2}) & \\ \quad + \sin(\frac{s}{2})(0.6197 + 0.0068\sin(s)) & \\ \quad + 0.1070\csc(\frac{s}{2})\sin^2(s), & s \in [\frac{\pi}{10}, \frac{3\pi}{20}], \\ \vdots & \\ 0.6197\cos(\frac{s}{2}) - 0.1426\cos^3(\frac{s}{2}) - 0.0046\sin^3(\frac{s}{2}) & \\ \quad + \sin(\frac{s}{2})(0.0047 + 0.2140\sin(s)) & \\ \quad + 0.0034\csc(\frac{s}{2})\sin^2(s), & s \in [\frac{17\pi}{20}, \frac{9\pi}{10}], \\ 0.6433\cos(\frac{s}{2}) - 0.1355\cos^3(\frac{s}{2}) - 0.0009\sin^3(\frac{s}{2}) & \\ \quad + \sin(\frac{s}{2})(0.0009 + 0.2033\sin(s)) + 0.0007\csc(\frac{s}{2})\sin^2(s), & s \in [\frac{9\pi}{10}, \frac{19\pi}{20}], \\ 0.6554\cos(\frac{s}{2}) - 0.1316\cos^3(\frac{s}{2}) + 1.9984 \times 10^{-15}\sin^3(\frac{s}{2}) & \\ \quad + 0.1974\sin(\frac{s}{2})\sin(s) - 1.3323 \times 10^{-15}\csc(\frac{s}{2})\sin^2(s), & s \in [\frac{19\pi}{20}, \pi], \end{cases}$$

and

$$U(s,1)=\begin{cases}4.4409\times 10^{-16}\cos(\frac{s}{2})-1.6653\times 10^{-16}\cos^3(\frac{s}{2})\\ \quad -0.1075\sin^3(\frac{s}{2})\\ \quad +\sin(\frac{s}{2})(0.5352+1.1102\times 10^{-16}\sin(s))\\ \quad +0.0806\csc(\frac{s}{2})\sin^2(s), & s\in[0,\frac{\pi}{20}],\\ 0.0008\cos(\frac{s}{2})-0.0008\cos^3(\frac{s}{2})-0.1107\sin^3(\frac{s}{2})\\ \quad +\sin(\frac{s}{2})(0.5254+0.0012\sin(s))\\ \quad +0.0830\csc(\frac{s}{2})\sin^2(s), & s\in[\frac{\pi}{20},\frac{\pi}{10}],\\ 0.0038\cos(\frac{s}{2})-0.0037\cos^3(\frac{s}{2})-0.1165\sin^3(\frac{s}{2})\\ \quad +\sin(\frac{s}{2})(0.5060+0.0056\sin(s))\\ \quad +0.0874\csc(\frac{s}{2})\sin^2(s), & s\in[\frac{\pi}{10},\frac{3\pi}{20}],\\ \vdots\\ 0.5061\cos(\frac{s}{2})-0.1165\cos^3(\frac{s}{2})-0.0037\sin^3(\frac{s}{2})\\ \quad +\sin(\frac{s}{2})(0.0038+0.1747\sin(s))\\ \quad +0.0028\csc(\frac{s}{2})\sin^2(s), & s\in[\frac{17\pi}{20},\frac{9\pi}{10}],\\ 0.5254\cos(\frac{s}{2})-0.1107\cos^3(\frac{s}{2})-0.0008\sin^3(\frac{s}{2})\\ \quad +\sin(\frac{s}{2})(0.0008+0.1660\sin(s))\\ \quad +0.0006\csc(\frac{s}{2})\sin^2(s), & s\in[\frac{9\pi}{10},\frac{19\pi}{20}],\\ 0.5352\cos(\frac{s}{2})-0.1075\cos^3(\frac{s}{2})+1.3322\times 10^{-15}\sin^3(\frac{s}{2})\\ \quad +0.1612\sin(\frac{s}{2})\sin(s)-8.8818\times 10^{-16}\csc(\frac{s}{2})\sin^2(s), & s\in[\frac{19\pi}{20},\pi],\end{cases}$$

respectively. Figure 1 displays the behavior of the numerical and exact solutions at different times. The graphs are in excellent affirmation. In Fig. 2 the absolute errors are presented in 2D and 3D at $t = 0.5$. Figure 3 demonstrates an excellent 3D contrast between the exact and numerical solutions at time step $t = 1$. In Table 1, a comparison of the error norms with those obtained in [22] is tabulated. Our methodology gives better precision for bigger τ over that obtained in [22]. The order of convergence is tabulated for the L_∞ norm in Table 2.

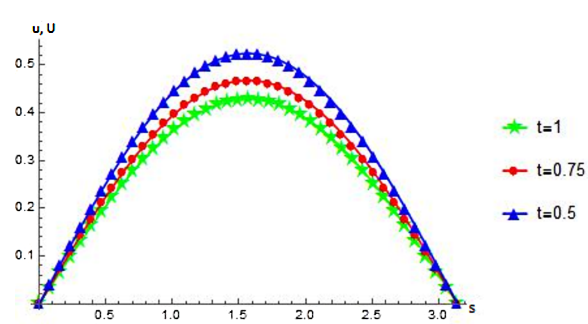

Figure 1 The exact (lines) and numerical (rectangles, stars, bullets) solutions for Example 1 when $\tau = 0.01$, $h = \frac{\pi}{80}$ at various time levels

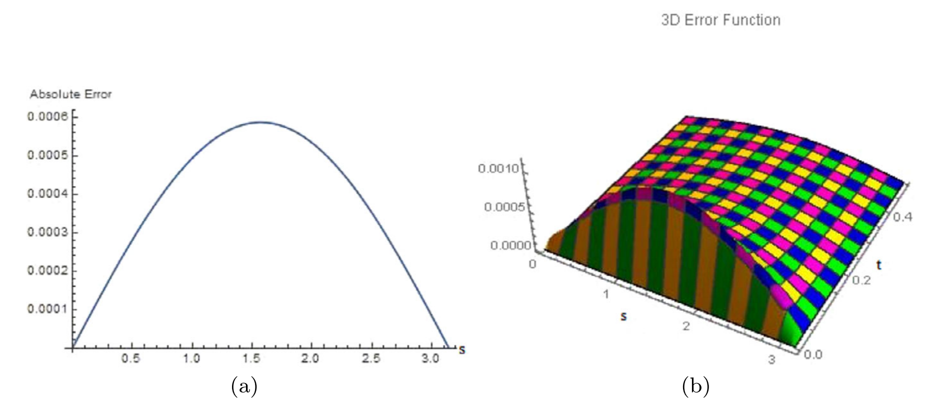

Figure 2 2D and 3D absolute error profiles when $\tau = 0.001$, $h = \frac{\pi}{60}$, $t = 0.5$ for Example 1

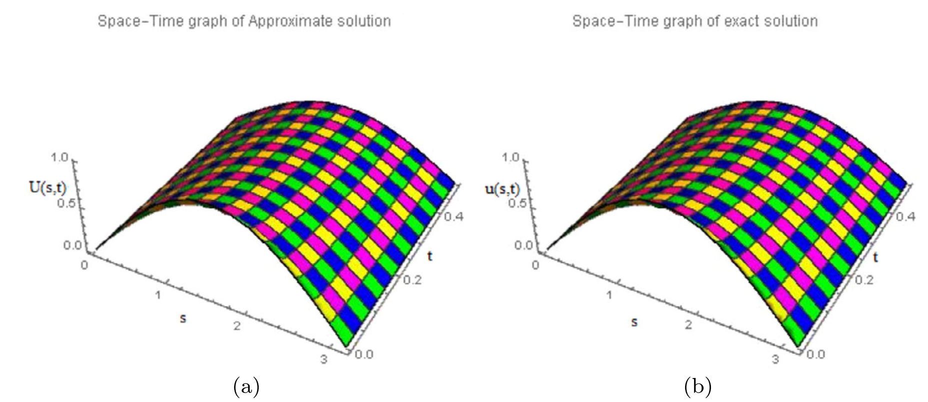

Figure 3 The exact (right) and numerical (left) solutions when $\tau = 0.001$, $h = \frac{\pi}{60}$, $t = 0.5$ for Example 1

Table 1 Comparison of error norms when $\gamma = 0.8$, $h = \frac{\pi}{M}$ for Example 1

M	GMMP Scheme [22] ($\tau = \frac{1}{9} \times 10^{-3}$)		Present Method ($\tau = 10^{-3}$)		
	L_2 Norm	L_∞ Norm	L_2 Norm	L_∞ Norm	CPU Time (s)
4	3.640e–02	5.426e–04	2.105e–02	1.679e–02	43.20
6	1.616e–02	4.331e–02	9.048e–03	7.219e–03	55.55
8	9.075e–03	1.136e–02	5.092e–03	4.063e–03	69.92
10	5.797e–03	7.304e–03	3.301e–03	2.634e–03	87.69
12	4.016e–03	5.080e–03	2.338e–03	1.865e–03	109.06
14	2.942e–03	3.732e–03	1.761e–03	1.405e–03	135.91
16	2.245e–03	2.854e–03	1.387e–03	1.107e–03	155.25
18	1.768e–03	2.252e–03	1.132e–03	9.032e–04	166.62
20	1.426e–03	1.820e–03	9.496e–04	7.577e–04	221.91
22	1.173e–03	1.500e–03	8.149e–04	6.502e–04	223.73
24	9.807e–04	1.257e–03	7.125e–04	5.684e–04	242.34
26	8.310e–04	1.067e–03	6.328e–04	5.049e–04	263.88
28	7.123e–04	9.169e–04	5.697e–04	4.545e–04	298.72
30	6.165e–04	7.955e–04	8.790e–05	4.139e–04	344.34

Table 2 Order of convergence for various values of M when $\tau = 0.001$, $\gamma = 0.8$ for Example 1

M	L_∞ Norm	OC	CPU Time (s)
2	9.253e–02	–	35.38
4	1.679e–02	2.462	43.20
8	4.063e–03	2.047	69.92
16	1.107e–03	1.876	155.25
32	3.810e–04	1.539	423.86

Example 2 Consider the nonhomogenous TFDE [22]

$$\begin{aligned} &{}_a^C D_t^{0.9} u(s,t) - \frac{\partial^2}{\partial s^2} u(s,t) \\ &\quad = \frac{2}{\Gamma(2.1)} t^{1.1} \sin(2\pi s) \\ &\qquad + 4\pi^2 t^2 \sin(2\pi s), \quad s \in [0,1], t \in [0,T], \end{aligned} \tag{29}$$

with zero initial and boundary conditions. This problem has the exact solution $u(s,t) = t^2 \sin(2\pi s)$.

We solve (29) by using the proposed scheme (11). The approximate solutions when $\tau = 0.01$ and $h = \frac{1}{20}$ at $t = 0.5$ and $t = 1$ are given by

$$U(s,0.5) = \begin{cases} 3.5527 \times 10^{-15} \cos(\frac{s}{2}) - 20.2482 \sin^3(\frac{s}{2}) \\ \quad + \sin(\frac{s}{2})(-57.6234 - 7.1054 \times 10^{-15} \sin(s)) \\ \quad + 15.1861 \csc(\frac{s}{2}) \sin^2(s), & s \in [0, \frac{1}{20}], \\ -0.1401 \cos(\frac{s}{2}) + 0.1310 \cos^3(\frac{s}{2}) \\ \quad - 18.3852 \sin^3(\frac{s}{2}) \\ \quad + \sin(\frac{s}{2})(-52.0206 - 0.20997 \sin(s)) \\ \quad + 13.7889 \csc(\frac{s}{2}) \sin^2(s), & s \in [\frac{1}{20}, \frac{1}{10}], \\ -0.6729 \cos(\frac{s}{2}) + 0.67101 \cos^3(\frac{s}{2}) \\ \quad - 14.8716 \sin^3(\frac{s}{2}) \\ \quad + \sin(\frac{s}{2})(-41.3734 - 1.0065 \sin(s)) \\ \quad + 11.1537 \csc(\frac{s}{2}) \sin^2(s), & s \in [\frac{1}{10}, \frac{3}{20}], \\ \vdots \\ 1.0159 \cos(\frac{s}{2}) + 0.6104 \cos^3(\frac{s}{2}) + 5.7332 \sin^3(\frac{s}{2}) \\ \quad + \sin(\frac{s}{2})(10.1455 - 0.9156 \sin(s)) \\ \quad - 4.2910 \csc(\frac{s}{2}) \sin^2(s), & s \in [\frac{17}{20}, \frac{9}{10}], \\ 25.0629 \cos(\frac{s}{2}) - 18.3491 \cos^3 -1.1608 \sin^3(\frac{s}{2}) \\ \quad + \sin(\frac{s}{2})(-45.5852 + 27.5236 \sin(s)) \\ \quad + 0.8707 \csc(\frac{s}{2}) \sin^2(s), & s \in [\frac{9}{10}, \frac{19}{20}], \\ 27.6261 \cos(\frac{s}{2}) - 20.1974 \cos^3(\frac{s}{2}) - 1.4323 \sin^3(\frac{s}{2}) \\ \quad + \sin(\frac{s}{2})(-50.5693 + 30.2961 \sin(s)) \\ \quad + 1.0742 \csc(\frac{s}{2}) \sin^2(s), & s \in [\frac{19}{20}, 1], \end{cases}$$

and

$$U(s,1)=\begin{cases}
-1.4211\times 10^{-14}\cos(\frac{s}{2})+3.5527\times 10^{-14}\cos^3(\frac{s}{2}) \\
\quad -80.9352\sin^3(\frac{s}{2}) \\
\quad +\sin(\frac{s}{2})(-230.33-2.8422\times 10^{-14}\sin(s)) \\
\quad +60.7014\csc(\frac{s}{2})\sin^2(s), & s\in[0,\frac{1}{20}], \\
-0.5600\cos(\frac{s}{2})+0.5595\cos^3(\frac{s}{2})-73.4887\sin^3(\frac{s}{2}) \\
\quad +\sin(\frac{s}{2})(-207.935-0.8393\sin(s)) \\
\quad +55.1165\csc(\frac{s}{2})\sin^2(s), & s\in[\frac{1}{20},\frac{1}{10}], \\
-2.6897\cos(\frac{s}{2})+2.6821\cos^3(\frac{s}{2})-59.4443\sin^3(\frac{s}{2}) \\
\quad +\sin(\frac{s}{2})(-165.376-4.0232\sin(s)) \\
\quad +44.5832\csc(\frac{s}{2})\sin^2(s), & s\in[\frac{1}{10},\frac{3}{20}], \\
\vdots \\
81.6459\cos(\frac{s}{2})-59.4851\cos^3(\frac{s}{2})-1.5295\sin^3(\frac{s}{2}) \\
\quad +\sin(\frac{s}{2})(-143.842+89.2276\sin(s)) \\
\quad +1.1471\csc(\frac{s}{2})\sin^2(s), & s\in[\frac{17}{20},\frac{9}{10}], \\
100.181\cos(\frac{s}{2})-73.3442\cos^3-4.6402\sin^3(\frac{s}{2}) \\
\quad +\sin(\frac{s}{2})(-182.211+110.016\sin(s)) \\
\quad +3.4802\csc(\frac{s}{2})\sin^2(s), & s\in[\frac{9}{10},\frac{19}{20}], \\
110.426\cos(\frac{s}{2})-80.7324\cos^3(\frac{s}{2})-5.7251\sin^3(\frac{s}{2}) \\
\quad +\sin(\frac{s}{2})(-202.134+121.099\sin(s)) \\
\quad +4.2938\csc(\frac{s}{2})\sin^2(s), & s\in[\frac{19}{20},1],
\end{cases}$$

respectively. We get the numerical results by utilizing the proposed scheme. A close comparison between the exact and numerical solutions at different times is shown in Fig. 4. In Fig. 5 the 2D and 3D error profiles are displayed at $t = 0.5$. Figure 6 deals with 3D comparison between the exact and approximate solutions. Table 3 reports a comparison of the error norms with those obtained in [22]. Although we have chosen a larger time step than that of [22], we still obtained a better accuracy. Table 4 records the convergence orders for the L_∞ norm.

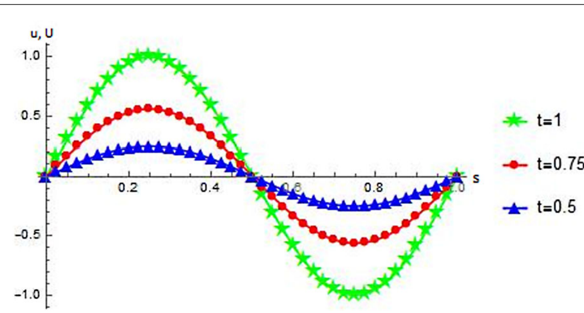

Figure 4 The exact (lines) and numerical (rectangles, stars, bullets) solutions when $\tau = 0.01$, $h = \frac{1}{80}$ at various time levels for Example 2

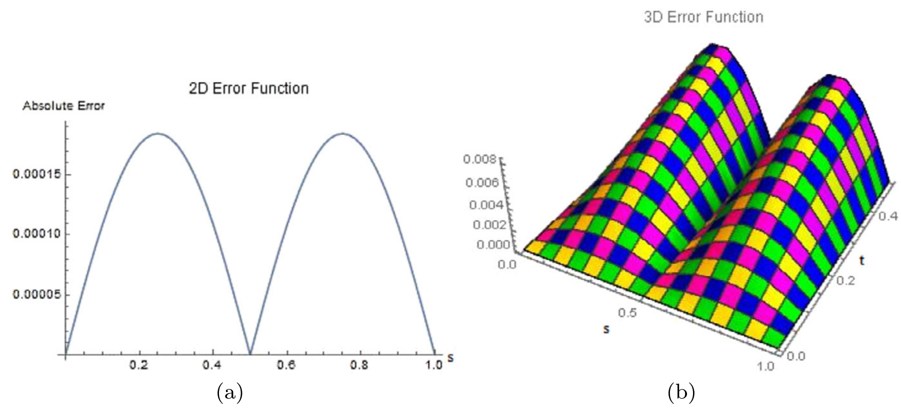

Figure 5 2D and 3D absolute error profiles when $\tau = 0.001$, $h = \frac{1}{60}$, $t = 0.5$ for Example 2

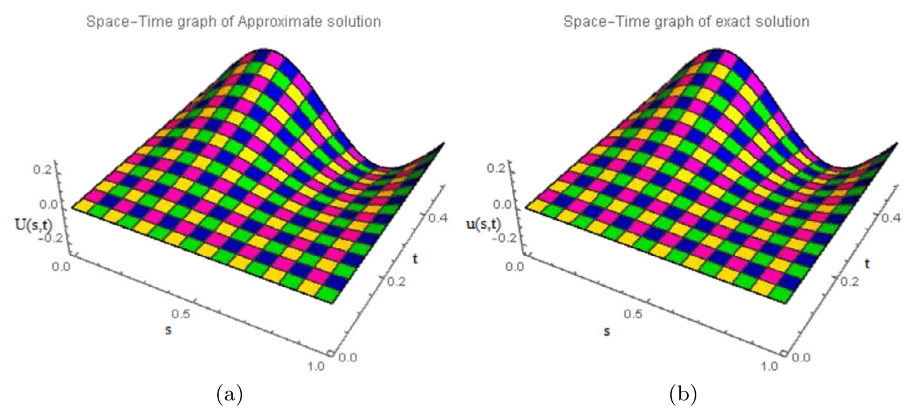

Figure 6 The exact (right) and numerical (left) solutions when $\tau = 0.001$, $h = \frac{1}{60}$, $t = 0.5$ for Example 2

Table 3 Comparison of error norms when $\gamma = 0.9$, $h = \frac{1}{M}$ for Example 2

M	GMMP Scheme [22] ($\tau = \frac{1}{12} \times 10^{-3}$)		Present Method ($\tau = 10^{-3}$)		
	L_2 Norm	L_∞ Norm	L_2 Norm	L_∞ Norm	CPU Time (s)
8	4.060e–02	9.248e–02	3.589e–02	4.339e–02	88.66
12	1.803e–02	4.303e–02	1.312e–02	1.935e–02	112.30
16	1.014e–02	2.459e–02	6.387e–03	1.086e–02	146.45
20	6.486e–03	1.585e–02	3.652e–03	6.947e–03	187.38
24	4.502e–03	1.104e–02	2.319e–03	4.831e–03	237.31

Table 4 Order of convergence for various values of M when $\tau = 0.01$, $\gamma = 0.9$ for Example 2

M	L_∞ Norm	OC	CPU Time (s)
8	4.460e–02	–	0.422
16	1.127e–02	1.9846	0.703
32	2.726e–03	2.0476	1.266
64	5.774e–04	2.2391	2.219

Example 3 Consider the TFDE describing subdiffusion [23]

$$\begin{aligned}\frac{\partial u(s,t)}{\partial t} &= {}_0D_t^{1-\gamma}\left[\frac{\partial^2 u(s,t)}{\partial s^2}\right]\\ &\quad + e^s\left[(1+\gamma)t^\gamma - \frac{\Gamma(2+\gamma)}{\Gamma(1+2\gamma)}t^{2\gamma}\right], \quad 0 < t \le 1, 0 < x < 1,\end{aligned} \tag{30}$$

with initial condition

$$u(s,0) = 0, \quad 0 \le s \le 1,$$

and boundary conditions

$$u(0,t) = t^{1+\gamma}, \qquad u(1,t) = et^{1+\gamma}, \quad 0 \le t \le 1.$$

This problem has the exact solution $u(s,t) = e^s t^{1+\gamma}$.

Following [24], equation (30) can be equivalently written as

$${}_0^C D_t^\gamma u(s,t) = \frac{\partial^2 u(s,t)}{\partial s^2} + e^s\left[\Gamma(2+\gamma)t - t^{1+\gamma}\right], \quad 0 < t \le 1, 0 < s < 1, \tag{31}$$

with same initial and boundary conditions. We apply scheme (11) to (30). The approximate solutions when $\tau = 0.01$, $h = \frac{1}{20}$, and $\gamma = 0.5$ when $t = 0.5$ and $t = 1$ are given by

$$U(s,0.5) = \begin{cases} 0.5744\cos(\frac{s}{2}) - 0.2208\cos^3(\frac{s}{2}) + 0.1593\sin^3(\frac{s}{2}) & \\ \quad + \sin(\frac{s}{2})(1.1850 + 0.3313\sin(s)) & \\ \quad - 0.1195\csc(\frac{s}{2})\sin^2(s), & s \in [0, \frac{1}{20}], \\ 0.5725\cos(\frac{s}{2}) - 0.2190\cos^3(\frac{s}{2}) + 0.1844\sin^3(\frac{s}{2}) & \\ \quad + \sin(\frac{s}{2})(1.2605 + 0.3284\sin(s)) & \\ \quad - 0.1383\csc(\frac{s}{2})\sin^2(s), & s \in [\frac{1}{20}, \frac{1}{10}], \\ 0.5685\cos(\frac{s}{2}) - 0.2150\cos^3(\frac{s}{2}) + 0.2106\sin^3(\frac{s}{2}) & \\ \quad + \sin(\frac{s}{2})(1.3398 + 0.3225\sin(s)) & \\ \quad - 0.1579\csc(\frac{s}{2})\sin^2(s), & s \in [\frac{1}{10}, \frac{3}{20}], \\ \vdots & \\ 0.0807\cos(\frac{s}{2}) + 0.2062\cos^3(\frac{s}{2}) + 0.6030\sin^3(\frac{s}{2}) & \\ \quad + \sin(\frac{s}{2})(3.0809 - 0.3093\sin(s)) & \\ \quad - 0.4522\csc(\frac{s}{2})\sin^2(s), & s \in [\frac{17}{20}, \frac{9}{10}], \\ 0.0039\cos(\frac{s}{2}) + 0.2637\cos^3(\frac{s}{2}) + 0.6159\sin^3(\frac{s}{2}) & \\ \quad + \sin(\frac{s}{2})(3.2400 - 0.3956\sin(s)) & \\ \quad - 0.4619\csc(\frac{s}{2})\sin^2(s), & s \in [\frac{9}{10}, \frac{19}{20}], \\ -0.0811\cos(\frac{s}{2}) + 0.3250\cos^3(\frac{s}{2}) + 0.6249\sin^3(\frac{s}{2}) & \\ \quad + \sin(\frac{s}{2})(3.4052 - 0.4874\sin(s)) & \\ \quad - 0.4686\csc(\frac{s}{2})\sin^2(s), & s \in [\frac{19}{20}, 1], \end{cases}$$

and

$$U(s,1)=\begin{cases} 1.6249\cos(\frac{s}{2})-0.6249\cos^3(\frac{s}{2})+0.4508\sin^3(\frac{s}{2}) \\ \quad +\sin(\frac{s}{2})(3.3515+0.9374\sin(s)) \\ \quad -0.3381\csc(\frac{s}{2})\sin^2(s), & s\in[0,\frac{1}{20}], \\ 1.6196\cos(\frac{s}{2})-0.6196\cos^3(\frac{s}{2})+0.5218\sin^3(\frac{s}{2}) \\ \quad +\sin(\frac{s}{2})(3.5652+0.9294\sin(s)) \\ \quad -0.3914\csc(\frac{s}{2})\sin^2(s), & s\in[\frac{1}{20},\frac{1}{10}], \\ 1.6083\cos(\frac{s}{2})-0.6084\cos^3(\frac{s}{2})+0.5959\sin^3(\frac{s}{2}) \\ \quad +\sin(\frac{s}{2})(3.7896+0.9126\sin(s)) \\ \quad -0.4469\csc(\frac{s}{2})\sin^2(s), & s\in[\frac{1}{10},\frac{3}{20}], \\ \vdots \\ 0.2280\cos(\frac{s}{2})+0.5835\cos^3(\frac{s}{2})+1.7062\sin^3(\frac{s}{2}) \\ \quad +\sin(\frac{s}{2})(8.7160-0.8753\sin(s)) \\ \quad -1.2796\csc(\frac{s}{2})\sin^2(s), & s\in[\frac{17}{20},\frac{9}{10}], \\ 0.01057\cos(\frac{s}{2})+0.7461\cos^3(\frac{s}{2})+1.7427\sin^3(\frac{s}{2}) \\ \quad +\sin(\frac{s}{2})(9.1663-1.1192\sin(s)) \\ \quad -1.3070\csc(\frac{s}{2})\sin^2(s), & s\in[\frac{9}{10},\frac{19}{20}], \\ -0.2298\cos(\frac{s}{2})+0.9195\cos^3(\frac{s}{2})+1.7682\sin^3(\frac{s}{2}) \\ \quad +\sin(\frac{s}{2})(9.6338-1.3793\sin(s)) \\ \quad -1.3261\csc(\frac{s}{2})\sin^2(s), & s\in[\frac{19}{20},1], \end{cases}$$

respectively. Figure 7 analyzes the graphs of the exact and approximate solutions when $\tau=0.01$ $h=\frac{1}{80}$, and $\gamma=0.5$. Figure 8 depicts the 2D and 3D error profiles, which exhibit exactness of the method. Figure 9 shows exceptionally close comparison of 3D graphs of approximate and exact solutions using $\tau=0.01$, $h=\frac{1}{60}$, and $\gamma=0.5$. In Tables 5–8 the maximum errors contrast with those presented in [23] for various values of τ and h to show that the present scheme is increasingly precise and gives better precision.

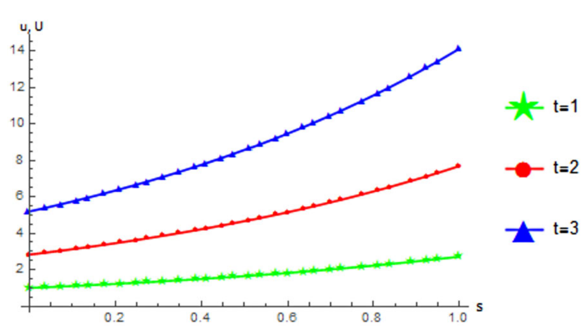

Figure 7 The exact (solid) and approximate solutions (stars, bullets, triangles) for Example 3 when $\tau=0.01$, $h=\frac{1}{80}$, and $\gamma=0.5$ at various time levels

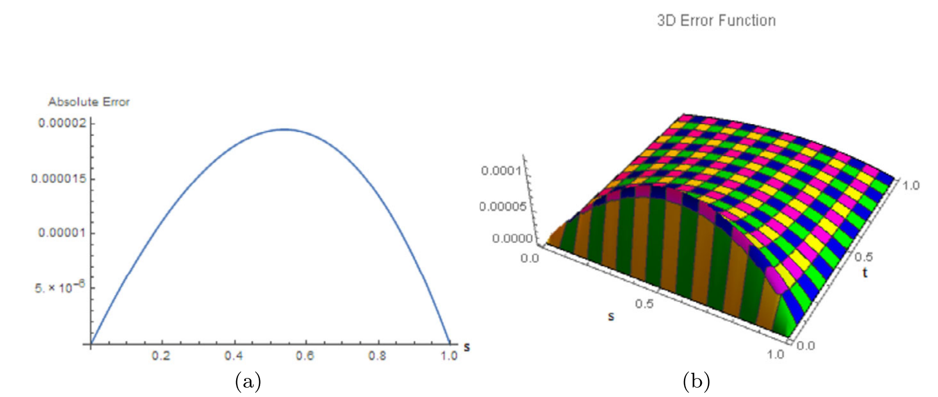

Figure 8 2D and 3D absolute error profiles when $\tau = 0.01$, $h = \frac{1}{60}$, $t = 1$ for Example 3

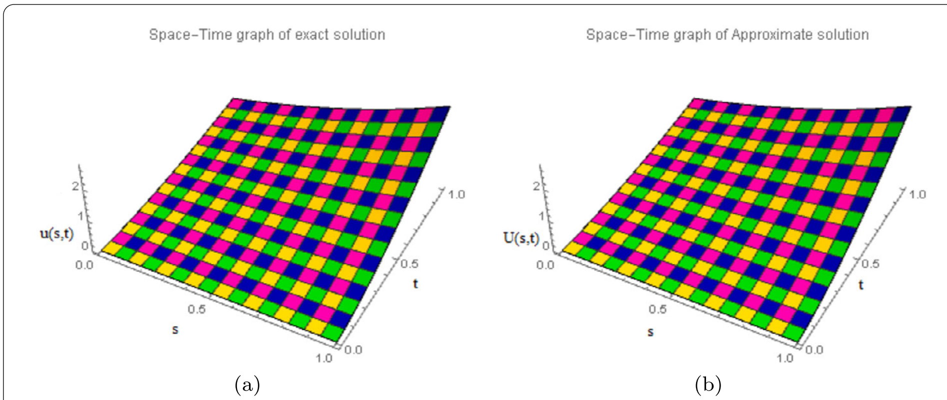

Figure 9 The exact (left) and numerical (right) solutions for Example 3 when $\tau = 0.01$, $h = \frac{1}{60}$, and $\gamma = 0.5$

Table 5 The maximum errors when $\tau = \frac{1}{64}$, $h = \frac{1}{8}$ for Example 3

γ	IDAS [23]	L_1-approximation [23]	Present Method	CPU Time (s)
0.4	0.9774769e–03	0.1812220e–02	0.959963e–03	0.230
0.5	0.1314691e–02	0.2103329e–02	0.908529e–03	0.239
0.6	0.1640956e–02	0.2363563e–02	0.803949e–03	0.220

Table 6 The maximum errors when $\tau = \frac{1}{1024}$, $h = \frac{1}{32}$ for Example 3

γ	IDAS [23]	L_1-approximation [23]	Present Method	CPU Time(s)
0.4	0.1204014e–03	0.2110046e–03	0.616098e–04	415.454
0.5	0.9040628e–04	0.01107985e–03	0.602786e–04	387.603
0.6	0.2180338e–03	0.2259971e–03	0.573334e–04	369.890

Table 7 The maximum errors when $\tau = h = \frac{1}{8}$ for Example 3

γ	IDAS [23]	Present Method	CPU Time (s)
0.4	0.5480236e–02	0.185967e–03	0.036
0.5	0.8357003e–02	0.639436e–03	0.037
0.6	0.1132181e–01	0.208645e–02	0.046

Table 8 The maximum errors when $\tau = h = \frac{1}{32}$ for Example 3

γ	IDAS [23]	Present Method	CPU Time (s)
0.4	0.1792436e–02	0.267127e–04	0.156
0.5	0.2493483e–02	0.142246e–03	0.156
0.6	0.3179647e–02	0.379025e–03	0.156

6 Conclusions

In this study, we developed a cubic trigonometric B-spline collocation method for numerical approximation of time-fractional diffusion equations. The time discretization is done using the typical finite difference method, whereas the derivatives in space are approximated by utilizing the trigonometric B-splines. The approximate solution is obtained as a piecewise continuous function, so that the solution can be approximated at any desired location in the domain of interest. We also presented a stability and convergence analysis of the scheme to affirm that the errors do not propagate. The obtained numerical results contrast with those of some current numerical procedures. We infer that the present scheme is more precise and provides better accuracy.

Acknowledgements
We thank Dr. Muhammad Amin for his assistance in proofreading of the manuscript. The authors are also grateful to anonymous referees for their valuable suggestions, which significantly improved this manuscript.

Funding
No funding is available for this research. We are grateful to Springer Open on providing full wavier for this manuscript.

Availability of data and materials
Not applicable.

Competing interests
The authors declare that they have no competing interests.

Authors' contributions
All authors equally contributed to this work. All authors read and approved the final manuscript.

Authors' information
Muhammad Yaseen is Assistant Professor; Muhammad Abbas and Muhammad Bilal Riaz are Associate Professors.

Author details
[1] Department of Mathematics, University of Sargodha, 40100 Sargodha, Pakistan. [2] Department of Mathematics, University of Management and Technology, 40100 C-II Johar Town Lahore, Pakistan. [3] Institute for Groundwater Studies (IGS), University of the Free State, 9300 Bloemfontein, South Africa.

Publisher's Note

Received: 14 July 2020 Accepted: 30 March 2021 Published online: 17 April 2021

References

1. Podlubny, I.: Fractional Differential Equations. Academic Press, San Diego (1999)
2. Mainardi, F.: Fractional calculus. In: Fractals and Fractional Calculus Continuum Mechanics, pp. 291–348. Springer, Berlin (1997)
3. Hilfer, R.: Applications of Fractional Calculus in Physics. World Scientific, Singapore (2000)
4. Sokolov, I.M., Klafter, J., Blumen, A.: Fractional kinetics. Phys. Today **55**, 48–54 (2002)
5. Diethelm, K., Freed, A.D.: On solution of nonlinear fractional order differential equations used in modelling of viscoplasticity. In: Scientific Computing in Chemical Engineering II: Computational Fluid Dynamics, Reaction Engineering and Molecular Properties, pp. 217–224. Springer, Heidelberg (1999)
6. Sokolov, I.M., Klafter, J., Blumen, A.: Ballistic versus diffusive pair-dispersion in the Richardson regime. Phys. Rev. E **61**(3), 2717–2722 (2000)
7. Chen, W.: A speculative study of $\frac{2}{3}$-order fractional Laplacian modeling of turbulence: some thoughts and conjectures. Chaos **16**, 23–26 (2006)
8. Metzler, R., Klafter, J.: The random walk's guide to anomalous diffusion: a fractional dynamics approach. Phys. Rep. **339**, 1–77 (2000)

9. Metzler, R., Klafter, J.: The restaurant at the end of the random walk: recent developments in the description of anomalous transport by fractional dynamics. J. Phys. A **37**(31), 161–208 (2004)
10. Iomin, A., Dorfman, S., Dorfman, L.: On tumor development: fractional transport approach. http://arxiv.org/abs/qbio/0406001
11. Metzler, R., Klafter, J.: Boundary value problems for fractional diffusion equations. Physica A **278**, 107–125 (2006)
12. Kilbas, A.A., Srivastava, H.M., Trujillo, J.J.: Theory and Applications of Fractional Differential Equations. Elsevier, Amsterdam (2006)
13. Langlands, T., Henry, B.: The accuracy and stability of an implicit solution method for the fractional diffusion equation. J. Comput. Phys. **205**, 719–735 (2005)
14. Esmaeili, S., Garrappa, R.A.: Pseudo-spectral scheme for the approximate solution of a time-fractional diffusion equation. Int. J. Comput. Math. **92**(5), 980–994 (2015)
15. Mustapha, K., Abdallah, B., Furati, K.M.: A discontinuous Petrov–Galerkin method for time fractional diffusion equations. SIAM J. Numer. Anal. **52**(5), 2512–2529 (2014)
16. Zhuang, P., Liu, F.: Implicit difference approximations for the time fractional diffusion equaition. J. Appl. Math. Comput. **22**(3), 87–99 (2006)
17. Karatay, I., Kale, N., Bayramoglu, S.R.: A new difference scheme for time fractional heat equations based on the Crank–Nicholson method. Fract. Calc. Appl. Anal. **16**(14), 892–910 (2013)
18. Yuste, S.B.: Weighted average finite difference methods for fractional diffusion equation. J. Comput. Phys. **216**, 264–274 (2006)
19. Yuste, S.B., Acedo, L.: An explicit finite difference method and a new von Neumann-type stability analysis for fractional diffusion equations. SIAM J. Numer. Anal. **42**(5), 1862–1874 (2005)
20. Murio, D.A.: Implicit finite difference approximation for time fractional diffusion equations. Comput. Math. Appl. **56**(4), 1138–1145 (2008)
21. Tasbozan, O., Esen, A., Yagmurlu, N.M., Ucar, Y.: A numerical solution to fractional diffusion equation for force-free case. Abstr. Appl. Anal. **2013**, Article ID 187383 (2013)
22. Huang, C., Yu, X., Wang, C., Li, Z.: A numerical method based on fully discrete direct discontinuous Galerkin method for the time fractional diffusion equation. Appl. Math. Comput. **264**, 483–492 (2015)
23. Chen, C.M., Liu, F., Turner, I., Anh, V.: A Fourier method for the fractional diffusion equation describing sub-diffusion. J. Comput. Phys. **227**, 886–897 (2007)
24. Gao, G., Sun, Z.: A compact finite difference scheme for the fractional subdiffusion equations. J. Comput. Phys. **230**, 586–595 (2011)
25. Abbas, M., Majid, A.A., Ismail, A.I.M., Rashid, A.: The application of cubic trigonometric B-spline to the numerical solution of the hyperbolic problems. Appl. Math. Comput. **239**, 74–88 (2014)
26. Prenter, P.M.: Splines and Variational Methods. Wiley, New York (1989)
27. De Boor, C.: A Practical Guide to Splines. Springer, Berlin (1978)
28. Siddiqi, S.S., Arshad, S.: Numerical solution of time-fractional fourth-order partial differential equations. Int. J. Comput. Math. **92**(7), 1496–1518 (2015)
29. Siddiqui, S.S., Arshad, S.: Numerical solutions of time-fractional fourth-order partial differential equations. Int. J. Comput. Math. **7**(92), 1496–1518 (2015)
30. Yaseen, M., Abbas, M., Ismail, A.I., Nazir, T.: A cubic trigonometric B-spline collocation approach for the fractional sub-diffusion equations. Appl. Math. Comput. **293**, 311–319 (2017)
31. Yaseen, M., Abbas, M., Nazir, N., Baleanu, D.: A finite difference scheme based on cubic trigonometric B-splines for time fractional diffusion-wave equation. Adv. Differ. Equ. **2017**, 274 (2017)
32. Yaseen, M., Abbas, M.: An efficient computational technique based on cubic trigonometric B-splines for time fractional Burgers' equation. Int. J. Comput. Math. **97**(3), 725–738 (2020)
33. Mohyud-Din, S.T., Akram, T., Abbas, M., Ismail, A.I., Ali, N.M.: A fully implicit finite difference scheme based on extended cubic B-splines for time fractional advection–diffusion equation. Adv. Differ. Equ. **2018**, 109 (2018)
34. Amin, M., Abbas, M., Iqbal, M.K., Baleanu, D.: Non-polynomial quintic spline for numerical solution of fourth-order time fractional partial differential equations. Adv. Differ. Equ. **2019**, 183 (2019)
35. Khalid, N., Abbas, M., Iqbal, M.K., Baleanu, D.: A numerical algorithm based on modified extended B-spline functions for solving time-fractional diffusion wave equation involving reaction and damping terms. Adv. Differ. Equ. **2019**, 378 (2019)
36. Akram, T., Abbas, M., Ismail, A.I., Ali, N.M., Baleanu, D.: Extended cubic B-splines in the numerical solution of time fractional telegraph equation. Adv. Differ. Equ. **2019**, 365 (2019)
37. Khalid, N., Abbas, M., Iqbal, M.K.: Non-polynomial quintic spline for solving fourth-order fractional boundary value problems involving product terms. Appl. Math. Comput. **349**, 393–407 (2019)
38. Amin, M., Abbas, M., Iqbal, M.K., Ismail, A.I., Baleanu, D.: A fourth order non-polynomial quintic spline collocation technique for solving time fractional super-diffusion equations. Adv. Differ. Equ. **2019**, 514 (2019)
39. Strikwerda, J.C.: Finite Difference Schemes and Partial Differential Equations, 2nd edn. SIAM, Philadelphia (2004)